A Look into the Cockpit of the Developing Locust: Looming Detectors and Predator Avoidance

Julieta Sztarker,[1,2] F. Claire Rind[1]

[1] Institute of Neuroscience, Newcastle University, Newcastle upon Tyne NE1 7RU, United Kingdom

[2] Departamento de Fisiología, Biología Molecular y Celular, FCEN, Universidad de Buenos Aires, IFIBYNE-CONICET, Pabellón 2 Ciudad Universitaria, Intendente Güiraldes 2160, Buenos Aires 1428, Argentina

ABSTRACT: For many animals, the visual detection of looming stimuli is crucial at any stage of their lives. For example, human babies of only 6 days old display evasive responses to looming stimuli (Bower et al. [1971]: Percept Psychophys 9: 193–196). This means the neuronal pathways involved in looming detection should mature early in life. Locusts have been used extensively to examine the neural circuits and mechanisms involved in sensing looming stimuli and triggering visually evoked evasive actions, making them ideal subjects in which to investigate the development of looming sensitivity. Two lobula giant movement detectors (LGMD) neurons have been identified in the lobula region of the locust visual system: the LGMD1 neuron responds selectively to looming stimuli and provides information that contributes to evasive responses such as jumping and emergency glides. The LGMD2 responds to looming stimuli and shares many response properties with the LGMD1. Both neurons have only been described in the adult. In this study, we describe a practical method combining classical staining techniques and 3D neuronal reconstructions that can be used, even in small insects, to reveal detailed anatomy of individual neurons. We have used it to analyze the anatomy of the fan-shaped dendritic tree of the LGMD1 and the LGMD2 neurons in all stages of the post-embryonic development of *Locusta migratoria*. We also analyze changes seen during the ontogeny of escape behaviors triggered by looming stimuli, specially the hiding response. © 2014 Wiley Periodicals, Inc. Develop Neurobiol 00: 000–000, 2014

Keywords: looming detection; LGMD; development; hiding; neuronal reconstruction

INTRODUCTION

The image of an approaching stimulus often signifies danger to an animal, and the ability to detect and respond appropriately to it can be crucial for survival.

Looming-sensitive visual neurons are known in several animals (pigeon: Sun and Frost, 1998; fish: Preuss et al., 2006; fruit fly: Fotowat et al., 2009; frog: Nakagawa and Hongjian, 2010) and have been particularly well studied in locusts where they were first described (Schlotterer, 1977; Rind and Simmons, 1992). Locusts possess a pair of large and uniquely identified visual neurons, the lobula giant movement detectors, LGMD1 (known mostly as LGMD) and LGMD2, which respond selectively to the images of an object looming toward the eye (Rind, 1987; Simmons and Rind, 1997). Extensive research has been done on the circuitry involved in looming detection and evasive behaviors in adult locusts (Rind and

Simmons, 1992; Simmons and Rind, 1992; Hatsopoulos et al., 1995; Gabbiani et al., 2002; Santer et al., 2005). The majority of this work has focused on the LGMD1 and on its postsynaptic neuron, the descending contralateral movement detector (DCMD; Rowell, 1971; Rind, 1984). However, additional neurons in the locust visual system also respond to looming stimuli and have been implicated in triggering evasive responses (Gray et al., 2010; Fotowat et al., 2011). The LGMD2 shares many key features with the LGMD1, including selective responses to looming stimuli, but it has been less often studied (Rind, 1987, 1996; Simmons and Rind, 1997) and neither its role in behavior nor its postsynaptic target neurons have been explored.

Almost all research on looming sensitive neurons has been done on adult locusts. Yet, in nature, locusts avoid predation throughout their lives. One of the earliest escape strategies locusts use, when sitting on a plant stem is hiding, by moving around the stem away from a looming stimulus (Hassenstein and Hustert, 1999). Because wings are not needed for this, both juveniles and adults could potentially perform this behavior although the hiding response has been studied only in 5th instars so far. Because hiding is triggered by looming stimuli, it could potentially involve the LGMD-DCMD system. The DCMD is already known to be involved in evasive behaviors: in controlling emergency glides and in different phases of the jump (Rind and Santer, 2004; Santer et al., 2005, 2006, 2008; Fotowat and Gabbiani, 2007).

Locusts follow a hemimetabolous pattern of development and grow gradually through post-embryonic development, so that, apart from the absence of functional wings, the juveniles share most of the physiological and morphological characteristics of the adults (Sehnal, 1985). The segmentally repeated pattern in the nervous system in hemimetabolous insects arises during early embryogenesis, as a stereotyped axonal scaffold upon which growth cones then fasciculate (Raper et al., 1983a, 1983b). Synapses form late in embryonic development (75%, Leitch et al., 1995) with specific partners in particular regions within the neuropils (Bastiani et al., 1984). The final structure of each neuron is not completely specified in the embryo: in locusts, mechano-sensory pathways established in the embryo can subsequently be modified during post-embryonic development, either by removal of the original target or by blocking activity (Pflüger et al., 1994). In the eye and optic lobe, where a continuous retinotopic map is established by the sequential ingrowth of receptor axons, precise connections are established gradually (Meinertzhagen,

1976). This gradual process extends throughout larval development in hemimetabolous insects and occurs rapidly during pupation which lasts 4 days in holometabolous ones like *Drosophila* (Heisinger et al., 2006). In the locust, new ommatidia are added at the anterior margin of the eye at each moult and receptors grow in to the lamina (Anderson, 1978). There, new synapses are formed with monopolar neurons which in turn will connect with columnar neurons in the medulla. These medulla neurons terminate in the lobula, one of their targets being the LGMD neurons. The new connections with the LGMD could either be formed between incoming neurons and newly extended fine distal LGMD dendrites or by a competition for existing space over an enlarged and fully branched neuron. In the last case, the main changes occurring during development would be an increase in the density of synapses without an obvious change in the dendritic organization of the LGMD. In adults, most input synapses are located on the fine processes of the LGMD1 and 2 (Rind and Simmons, 1998).

The stereotyped anatomy of the insect optic lobe, which has a high degree of invariance in identified neurons between different individuals, suggests that visual experience does not play a major role in shaping the circuits in the visual system. However, early visual experience has an effect on the size of the optic lobes in *Drosophila* (Barth et al., 1997) and synapse numbers in other flies (Rybak and Meinertzhagen, 1997). This effect is mainly at the level of the receptor cells, and in the lobula region of the fly optic lobe visual experience was found to have no influence on the anatomy of the directionally selective tangential cells (Karmeier et al., 2001).

Studying the development of the DCMD neuron Bentley and Toroian-Raymond (1981) found that by 80% of embryonic development the adult arborization pattern of the DCMD was already established. Although the post-embryonic development of the LGMD1 neuron has not been studied directly, we have recently shown that the 1st instar DCMD neuron, postsynaptic to the LGMD1 is already able to respond to approaching objects although its selectivity and intensity of response both increase during postembryonic development (Simmons et al., 2013). Which changes in the LGMD1 dendritic tree structure accompany this improvement is not known.

Here, we decided to study in detail the changes undergone during postembryonic development by two neurons with established relevance in looming detection. In adults, intracellular staining is normally used for morphological characterization of the LGMD neurons (O'Shea and Williams, 1974; Rind, 1987; Simmons and Rind, 1997; Rind and Simmons,

1998; Peron et al., 2007). Using the same methods in young instars would be difficult especially considering newly hatched locusts have heads about 1 mm long. Instead, we used a technical approach combining classical staining techniques and 3D neuronal reconstructions that allowed the characterization of the anatomy of the LGMD1 and 2 neurons in the lobula throughout postembryonic development, from the newly hatched 1st instar to the last larval instar, the 5th. We performed a morphometric analysis to evaluate the changes produced in the two neurons during postembryonic development. We also describe the accompanying modifications, occurring through ontogeny, in the performance of escape responses shown by unrestrained locusts positioned on a rod, to either real, or computer generated, looming stimuli.

MATERIALS AND METHODS

We used male and female 1st to 5th larval instars and adults of *Locusta migratoria*, taken from a gregarious laboratory culture kept at 30°C, with a 12:12 h light-dark cycle. Eggs were laid in sand-filled pots. Instar was determined by measuring the size of the body and wing buds and by comparing the shape of the pronotum with reference measurements we made in carefully staged locusts. First instar hoppers were used between 1 and 12 h of hatching from the egg.

Neuronal Reconstruction

Intracellular staining in adult locusts has shown previously that both LGMD neurons are large, relatively invariant in shape between individuals and occupy a relative consistent position in the lobula (Rind and Simmons, 1998; Rind and Leitinger, 2000; Peron et al., 2007). In toluidine blue stained sections through the brain, LGMD1 and LGMD2 are readily recognizable in the distal lobula because their processes are considerably wider in diameter than those belonging to other neurons. They are arranged in two crescents, the processes of the LGMD2 located nearer to the posterior brain surface than those of the LGMD1 (Rind and Leitinger, 2000). Accordingly, the lobula arborizations of the two neurons were easily recognized and distinguished in reduced silver preparations in all instars as well as in adults [Fig. 1(A)]. We used Bodian's reduced-silver method (following the protocol described in Sztarker et al., 2005). Briefly, after cold anesthesia, locust's heads were cut off, mandibles removed, and a window opened in the cuticle in the back of the head to allow rapid fixation. Brains were fixed for 6 h in AAF (5% glacial acetic acid, 85% ethanol, 10% formalin). After washing, brains were dissected out of the head, dehydrated, and mounted in Paraplast plus (TAAB laboratories Equipment, Berkshire). Blocks were serially sectioned at 12 μm. Dewaxed sections were incubated overnight at 45°C in 250 mL distilled water containing 1% silver proteate (Johnson Matthey SA, London) and 1–2 g clean copper turnings (Fisher Scientific UK, Leicestershire) per 100 mL solution. After incubation, tissue was placed in developer, gold toned, reduced, and then fixed. Following dehydration, sections were mounted in Histomount (Fisher Scientific UK, Leicestershire) under coverslips. LGMD profiles were identified using an Olympus BH-2 microscope and then were traced in several successive 12 μm sections (4–12 sections depending on animal size) using Neurolucida software (MBF bioscience, Williston, VT) as detailed in the results section to generate three-dimensional reconstructions of the neurons.

We used NeuroExplorer (MBF bioscience, Williston, VT) to analyze structural changes in the LGMD1 and LGMD2 neurons during postembryonic development. We quantified the length and the number of segments constituting each dendritic tree. Then, by analyzing the branch order of each segment, we obtained the maximum branch order and plotted branching pattern histograms for the frequency of each order of branch. We additionally analyzed the data derived from the segment analysis of the dendritic tree structures of LGMD1 and LGMD2 neurons using a canonical discriminant analysis (CDA) in four of the five instars using SPSS v19 (IBM Statistics, Armonk, NY). We used the anatomical details of 15 LGMD neurons in total, 8 LGMD1 and 7 LGMD2: 2 LGMD1 and 2 LGMD2 from each of the 1st and 2nd instars; 3 LGMD1 and 2 LGMD2 from the 4th instars; and 1 LGMD1 and 1 LGMD2 from 5th instar locusts.

In some subjects, data were from the same individual, in others, as in the 1st instar, LGMD1 and 2 were from separate individuals but were closely matched in size as these were 1-day old (3rd instars were not included because there were size differences between the individuals from which LGMD1 and LGMD2 were reconstructed). We used this analysis to quantify the changes produced in each of these neurons during development and to identify which structural parameters could be used to categorize them. It also provided a distance measure to have a quantitative index of similarity. We tested the following metrics, defined as in Figure 1: x, y, and z co-ordinates of each branch point, the order of each branch in the dendritic tree, the change in xy and z angle of each branch compared with the lower order branch, from which it arises (the last two represent the spherical coordinate angles for the end of a segment relative to the start of the next segment). Coordinates reflect the shape of each neuron and relate to natural head and body axes: z corresponds to the anterior-posterior axis, x to the dorso-ventral, and y to the proximal-distal. Because the LGMD2 is located posteriorly to the LGMD1, nearer to the hind surface of the optic lobe, when both neurons were reconstructed from the same optic lobe the z values of the LGMD 2 are more positive than those for the LGMD1.

Hiding Behavior

For our initial series of behavioral experiments, we used a real object looming toward the animal to elicit escape
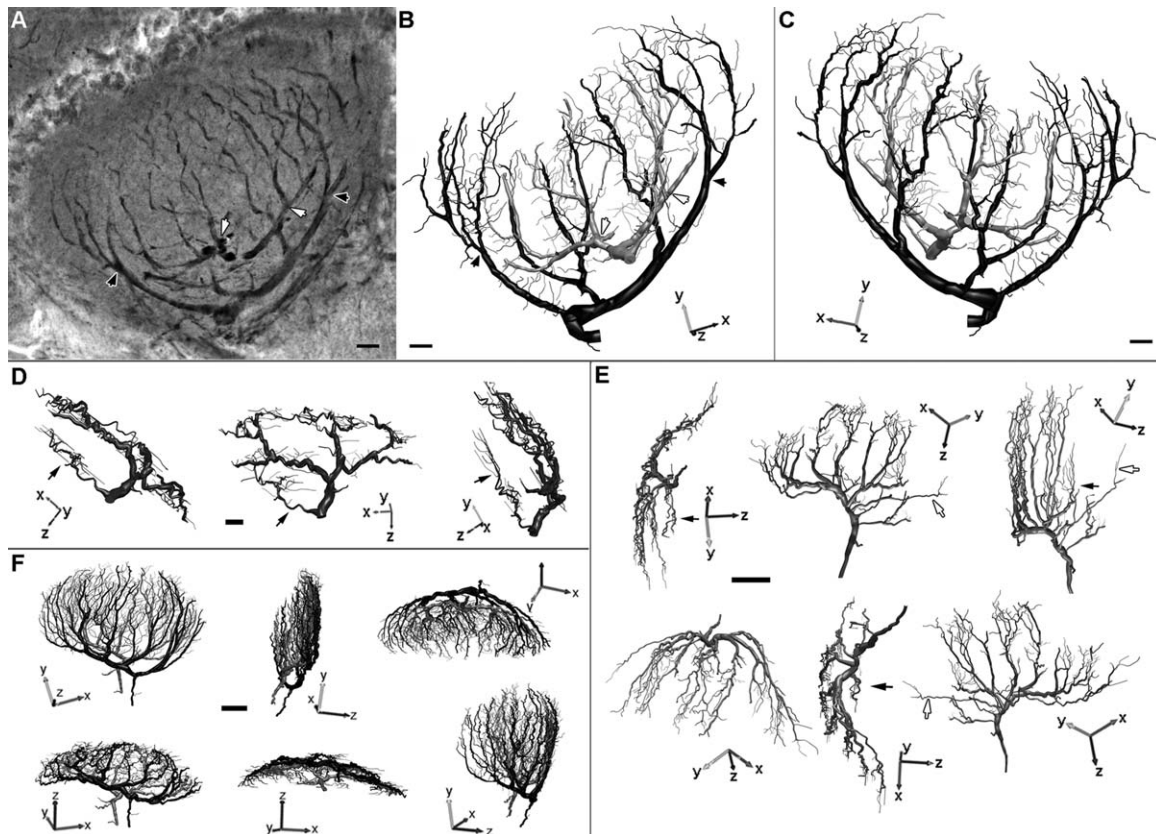
Figure 1 Three-dimensional neuronal reconstructions of the LGMD1 and the LGMD2 from Bodian-stained brains. A: Photo-montage of a lobula (2nd instar) stained with Bodian's method obtained from images of 5 consecutive 12 μm sections that were made transparent, aligned and then flattened in Photoshop. B: Reconstructions derived from the same preparation as (A), made using Neurolucida. To aid understanding, points belonging to the LGMD1 (white arrowheads) and to the LGMD2 (black arrowheads) that correspond in (A) and (B) are marked. C: Stereo image of the same reconstructed neurons showed in B but rotated 180°. D: Three different views of the 2nd instar LGMD1 shown in (B) where a second dendritic field (subfield B, black arrows) in addition to the main one is evident. E: Six different views of a 4th instar LGMD1 showing the smaller dendritic subfields B (black arrows) and C (white arrows) in addition to subfield A. F: Six different views of the LGMD1 and 2 neurons reconstructed in a 5th instar showing the contiguity of the dendritic trees. Anatomical coordinates defined relative to the head: x: dorso-ventral, y: Proximo-distal, z: anterio-posterior. Scale bar: 10 μm in (A–C); 50 μm in (D) and (E).

responses. The looming stimulus consisted of a 10 cm diameter black Styrofoam ball approaching along a 1 m rail (inclination 2.2°). The approach took 2.3 s, with an initial object subtense on the eye of 5.4°, a final subtense of 79.6° giving an overall l/v value of 115 ms, assuming a constant velocity of 0.44 m/s. In fact as the ball rolls down the incline, it will be subject to an acceleration component due to gravity (0.38 m/s^2 calculated using uniform accelerated rectilinear motion formulae), giving a final velocity of 0.874 m/s. We selected a slow approach to bias responses toward hiding. Faster approaching stimuli (steeper inclination) produced a higher number of jumping responses.

Two metal rings with a motion detector attached documented the passing of the ball just after the release and near the end of the trajectory [1 m apart, white arrowheads in Fig. 2(A)]. When the ball passed each detector an LED was illuminated. The two LEDs were filmed along with the locusts to synchronize the response with the passage of the stimulus. The ball was held in place and then released by a long stick that was moved gently [Fig. 2(B)], with a movement that did not trigger any response from the locust in the absence of a ball. The locust sat on a vertical wooden rod in a head-up posture. We used a different rod size for each instar, maintaining a similar proportion between the size of animal and rod (diameter: 2.5 mm for 1st and 2nd instars, 4 mm for 3rd, 6 mm for 4th, 7 mm for 5th and 9 mm for adults). Animals were unrestrained. They were placed perpendicular to the trajectory of the ball and viewed the ball only with the right eye. Locusts were first left undisturbed for 5 min and then three trials, separated
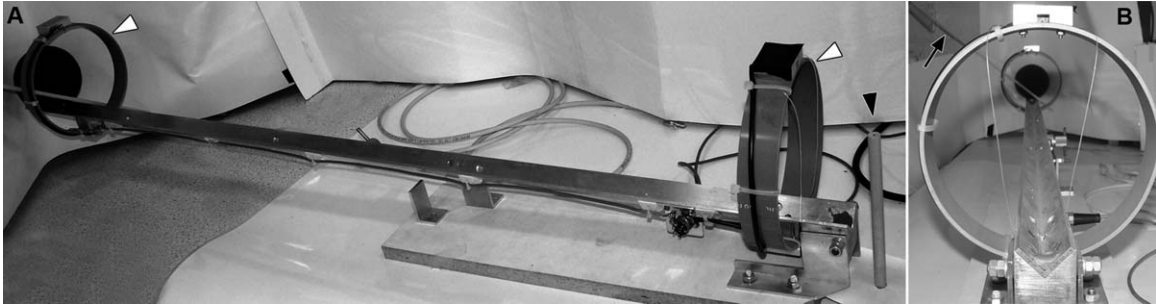
Figure 2 Setup for behavioral experiments using a real ball. A: We used a 10 cm diameter black Styrofoam ball that rolled along a 1 m rail (inclination 2.2°). Locusts sat on the top of a wooden rod proportional to their size (black arrowhead). Two metal rings each containing a motion detector monitored the passing of the ball: soon after release and near the end of the trajectory (white arrowheads). B: Locust's point of view. The ball was set free remotely by the smooth movement of a long stick (black arrow).

by 5 min intervals, were conducted with each animal. Responses were filmed from above with a JVC GR-D290EK digital video camera at a resolution of 30 frames/s and analyzed off-line.

After classifying the response in a video recording (see Results), videos were analyzed frame by frame using the program "Imaging MotionScope" (Redlake, San Diego, CA). We determined: (a) the frame before the one in which movement of the locust was first detected (initial position, IP); (b) the frame in which the furthest rotational position relative to the original position was reached (FP, final position); (c) the latency of response, calculated as the time between the ball passed through the first metal ring (the first LED turned on) and the IP; (d) the angle through which the locust had rotated, calculated using the program ImageTool (UTHSCSA, San Antonio, TX) to measure the angle formed by the positions of the midline of the locust on the frames IP and FP relative to the center of the rod; and (e) the initial (fastest) velocity, calculated as the angle rotated during the first 66–200 ms of the response. The interval chosen depended on the actual response of the locust: by repeated careful observation of each video, we separated the first, rapid component, from the next, slower part of the response to calculate the maximum rotation velocity achieved.

Locusts that repeatedly jumped as a response were discarded (less than 5% of the animals). This stimulus was very effective in generating behavioral responses in locusts (we recorded active responses in 99.5% of the trials).

For our second series of behavioral experiments, we used computer-generated stimuli to trigger hiding in locust. We used different combinations of velocities (0.25, 0.5, 1, 1.5 ms^{-1}) and sizes (8.5 and 15 cm diameter) to stimulate 5th instar locusts and selected a 15 cm diameter dark disk that loomed at 0.25 ms^{-1}, starting 1.55 m from the locust as the more effective for triggering hiding responses. This gave an approach with an $l/|v|$ ratio of 300 ms, where l is object radius and $|v|$ is approach velocity (Gabbiani et al., 2002). We used dark and light stimuli. The contrast of the looming

stimulus against the background, defined as (object intensity-background intensity)/background intensity, was 0.8 (background illuminance, measured at the screen with a "Tecpel 530" light meter was 265 lux; the dark disk had an illuminance of 74 lux and the light disk of 456 lux). A locust sat vertically on a rod 6 cm from the screen and viewed the image expansion with the right eye. Stimuli were displayed on a 20 inch, Clinton Monoray monitor from Cambridge Research Systems, with a fast greenish-yellow phosphor (DP104) and a refresh rate of 150 Hz. Looming stimuli were generated using a Cambridge Research Systems VSG2/5B graphics card in a Dell Optiplex GX260 computer. We used 1st, 3rd, and 5th instars (10 locusts in each group). Each animal was left undisturbed for 5 min and then was subject to six trials separated by 3 min, three with a dark and three with a light disk, presented in a random order. Responses were filmed from above and analyzed off-line as before. For timing the responses, the end of the stimulus approach could be seen in the videos. Some additional trials (not used for analyzing locust responses) were recorded in which a mirror enabled us to capture the complete stimulus dynamic into the recorded frame.

We performed a control experiment with nine additional 3rd instars to verify that the locusts were responding to the actual loom and not to the accompanying luminance change. We stimulated each locusts with a set of three or more trials with the dark looming stimulus, then a set of three trials with static equivalent luminance decrease stimuli and then again to a set of three trials with the dark looming stimulus. Responses to each stimulus were videoed and quantified. The inter-trial interval was at least 3 min.

All behavioral experiments were conducted at a room temperature of 24–25°C.

Data Analysis

Statistical tests on the hiding responses were performed using SPSS (IBM Statistics, Armonk, NY). When possible,

we used ANOVA (one-way and repeated measures) to analyze the data. When unequal variance between groups was found, we used Welch's Robust ANOVA.

RESULTS

Development of the LGMD Neurons

To study the morphology of the LGMD1 and LGMD2 neurons in all the postembryonic stages of locust development, we used a new neuronal reconstruction approach. We used Neurolucida software for making three-dimensional reconstructions but instead of using it to reconstruct a cell from a single stained preparation, we used it on generally stained (Bodian) sections. Even though this reduced silver method is unspecific, some parameters, such as the copper concentration, can be increased to stain only a small fraction of the neuronal processes including usually wide-field tangential neurons (Sztarker et al., 2005). Under these conditions, the main and most characteristic branches of the LGMD1 (belonging to subfield A, see below) and of the LGMD2 in the lobula were easily identified and distinguished from each other by their location in these preparations [Fig. 1(A)]. We began the reconstructions from a 12 μm section in which some of these distinctive branches appeared, drew the branches contained in all the possible focus planes through that section, using a motorized z drive to record the depth of each feature in the section, and then reconstructed the rest of the neuron following the continuation of each branch, in consecutive sections. When moving from one section to the next, external cues (e.g., the border of the neuropils, tracheae, etc.) were used to reorient the drawing. If there was no obvious continuity between branches, we still drew the candidate branches and decided afterward if they belonged to the dendritic tree. In those cases, we either erased the branch afterward or used the editing tools from Neurolucida to join branches if it was decided that they belonged to the same neuron. This decision was based solely on the proximity of the beginning of the unattached branch to the rest of the dendritic tree (in *x, y,* and *z* axes) as viewed in the 3D rotating model produced by the software. Supporting Information Movie 1 shows an example from an ongoing reconstruction of a 4th instar LGMD2 in which the three unattached green branches are evidently part of the same dendritic tree, whereas the red ones belong to a different neuron.

Due to the physical separation between the two neurons, in most cases both LGMD1 and LGMD2 could be reconstructed at the same time. With this painstaking procedure, even small branches (about 0.5 μm) could be assigned to a neuronal tree [Fig. 1(B,C)]. Examples of 3D reconstructions of LGMD neurons seen in different views in a 2nd, 4th, and 5th instar are shown in Figure 1(D–F) (Supporting Information Movies 2–3). Because there are already numerous accounts showing the morphology of the LGMD neurons in adults (e.g.,: O'Shea and Williams, 1974; Rind, 1987; Simmons and Rind, 1997; Rind and Simmons, 1998; Peron et al., 2007) and because as the animal grows neuronal reconstruction becomes more demanding and difficult with this method, we did not include adults in our study. Nevertheless, our 5th instar reconstruction of the two LGMDs have very similar morphological features when compared with the same neurons intracellularly stained in an adult [Fig. 3(A,B)]. Several reconstructions were made for each neuron type and instar. In this analysis, we considered only the ones where the complete fan-shaped tree was reconstructed (one to three in each category). The reconstruction method was reliable because comparing the morphology of two different reconstructions, in different locusts of the same developmental stage, produced similar results for the different parameters measured in the final reconstructed neurons [e.g.,: total dendritic surface, segment number and mean length, highest branch order, etc.; Fig. 3(C,D)].

In the adult locust, intracellular staining had previously shown that the arborization of the LGMD1 in the lobula consists of three different dendritic subfields, the most prominent is the fan-shaped subfield A which receives excitatory inputs from medulla columnar elements, the other two, subfields B and C, receive inhibitory inputs (O'Shea and Williams, 1974). The LGMD2 possesses one fan-shaped dendritic field in the lobula, located almost parallel but closer to the surface of the brain, and surrounding the subfield A of the LGMD1 (Rind, 1987; Simmons and Rind, 1997; Rind and Leitinger, 2000). In most cases, we were able to reconstruct the subfield B of the LGMD1 [Fig. 1(D,E)]. The subfield C was more elusive [but see Fig. 1(E)] probably because of the orientation of the thin and long process that connects it to the principal tree that make it difficult to follow through the sections. For the subsequent quantitative analysis, we took into account only the subfield A of the LGMD1. An example of a complete reconstruction of the fan-shaped tree of an LGMD1 and an LGMD2 is displayed in Figure 4 for each developmental stage. The overall shape (outline) of the LGMD1 and the LGMD2 is similar in all instars. In the two neurons, the fan-shaped arborization is made up of several principal branches of wide diameter
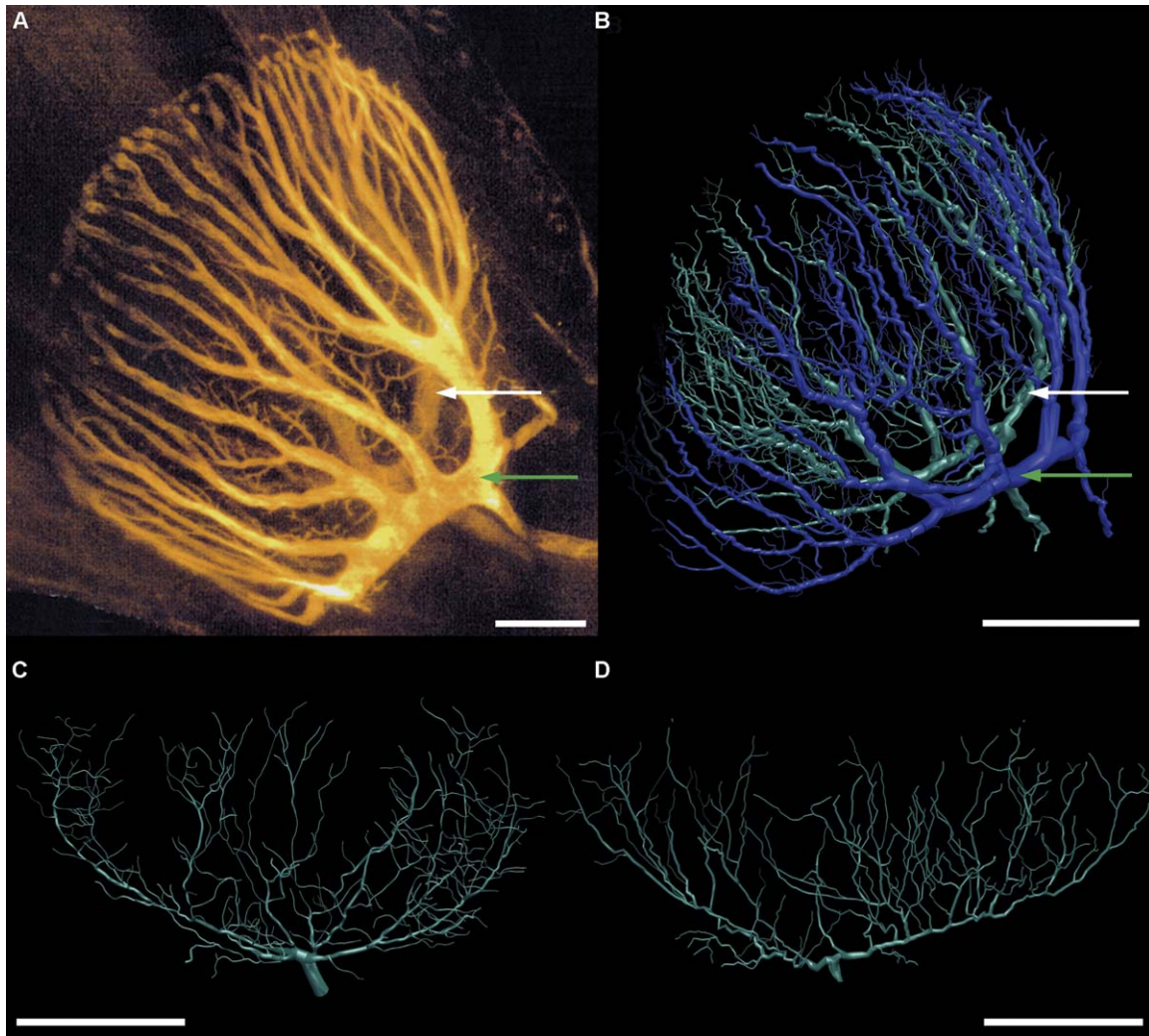
Figure 3 Validity of the reconstruction method. Comparison between a confocal reconstruction of the two LGMD neurons stained intracellularly in an adult (A) and a Bodian based Neurolucida reconstruction of the same neurons in a 5th instar (B). White arrows point to the LGMD1 and green arrows to the LGMD2. C and D: Two examples of the LGMD2 neuron reconstructed from two different 1st instar locusts. Scale bar: 50 μm.

(they are numbered in the 5th instar examples in Fig. 4). A branch is designated as principal when it arises directly from the principal neurite or, occasionally, when it arises by bifurcation from a branch originating from the principal neurite that gives rise to two wide processes of similar diameter (each of them constituting therefore a principal branch). The other inclusion criterion is that each principal branch has to give rise to an extensive arborization occupying a substantial portion of the dendritic field. The latter is more evidently appreciated in the rotating 3D model of the neuron. Therefore, the number of principal branches in an LGMD was ultimately established on examining the reconstructed neuron with the 3D visualization tools in the Neurolucida software. The number obtained was comparable in all juveniles [Fig. 5(A)] and similar to the number described in adults (7–10 dendrites; O'Shea and Williams, 1974; Simmons and Rind, 1997). Nonetheless, trees do become bigger and more complex as locusts grow. We used the NeuroExplorer tools to quantify this. We chose parameters that have been used before to quantify dendritic changes through development (Libersat and Duch, 2002). We used a "color by branch" analysis in which each segment is colored according to its centripetal order in the tree [each order uses a unique color, see Fig. 5(B); a segment is defined as a portion of a branched structure that is delimited by nodes or terminations with no intermediate nodes]. We analyzed the length and order of each segment in a tree.
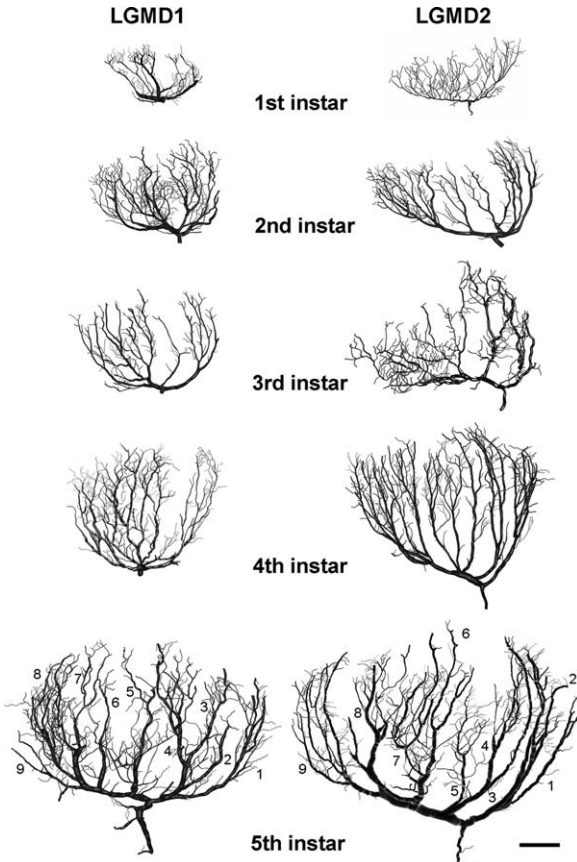
Figure 4 Presence and development of LGMD1 and LGMD2 in all instars. An example of a complete reconstruction of each neuron in all nymphal stages is shown. They are all displayed in a frontal view and at the same scale. The axes (*x, y*, and *z*) are defined relative to the locust's head. In the 5th instar reconstructions, the principal branches contained in the fan-shaped arborization are indicated by successive numbers. Regardless of minor differences caused by the original orientation of the sections from which the neurons were reconstructed, some of these branches are easily identifiable in all the other instars. Scale bar: 50 μm.

Larval development was accompanied by an increase in the total length of segments in the fan-shaped arborization [Fig. 5(C)]. As can be seen in Figures 5(D,E), this increase was mainly due to an increase in the number of segments because the mean segment length did not change dramatically with instar stage. To compare the overall shape of the trees, we made a branch order analysis showing the distribution of segments in the different branch orders [Fig. 5(F)]. In both LGMD neurons, 1st to 4th instars showed a similar distribution of branches, changing mainly in the number of branches in each order. On the other hand, 5th instars showed a wider distribution and a shift toward branches with higher orders. This same tend-

ency is shown in Figure 5(G) displaying the maximum order reached by the branches of the LGMD1 and the LGMD2 in each developmental stage.

Data derived from the segment analysis of the LGMDs, obtained using NeuroExplorer, were also used to assess the developmental differences in the structure of the neurons in a systematic way using CDA. CDA is used to find the maximal co-linearity between a set of variables that predicts group membership (Rencher, 1992; Wright et al., 2005). CDA revealed that the ratio of the structural features of the LGMD1 and 2 neurons could be used to identify which instar the neuron belonged to (Table 1). For each neuron, we obtained three discriminant functions (Table 1, second row), each a combined linear weighting of the anatomical measurements. Taken together, these functions separated LGMD1 and 2 neurons of each of the 4 instars into statistically significant categories that corresponded to the instars (see below). For the LGMD1, the first discriminant function of the CDA explained 92.7% of the variance in the data (Table 1, left columns). The biggest differences for the LGMD1 neuron occurred at the transition from 4th to 5th instar. The 5th instar LGMD1 neuron was the most distinct and was easily separated from all the other instars in the CDA by information about the negative relationship between the *Y* and *Z* coordinates of their branch points and by the sign of discriminant function 1 (Table 1, CDA: $\chi^2_{18} = 4037$, $p < 0.001$). The second discriminant function separated the 1st instar from the 2nd and 4th instars using neuronal branch order as the most important morphological trait for this separation (Table 1, CDA: $\chi^2_{10} = 466$, $p < 0.001$). The 2nd and 4th instar LGMD1 neurons could be distinguished simply by the correlation between the *Y* and *Z* coordinates; in the 2nd instar, there was a greater difference in *Y* and *Z* than in the 4th instar (Table 1, CDA: $\chi^2_4 = 175$, $p < 0.001$).

The LGMD2 neurons (Table 1, right columns) also grew more distinct as the locusts aged. The 5th instar LGMD2 neuron was separated from all the other instars in the CDA by the first discriminant function with its strong relationship between the *X* and *Y* coordinates of each branch point and with branch order (Table 1, CDA: $\chi^2_{18} = 2534$, $p < 0.001$). The second discriminant function separated the 4th instar from the 1st and 2nd instars using a combination of morphological features, with only the *Z* angle not being important (Table 1, CDA: $\chi^2_{10} = 1332$, $p < 0.001$). The 1st and 2nd instar LGMD2 neurons were distinguished mainly by the higher branch order in the 2nd instar neurons and the *XY* angle (Table 1, CDA: $\chi^2_4 = 374$, $p < 0.001$).
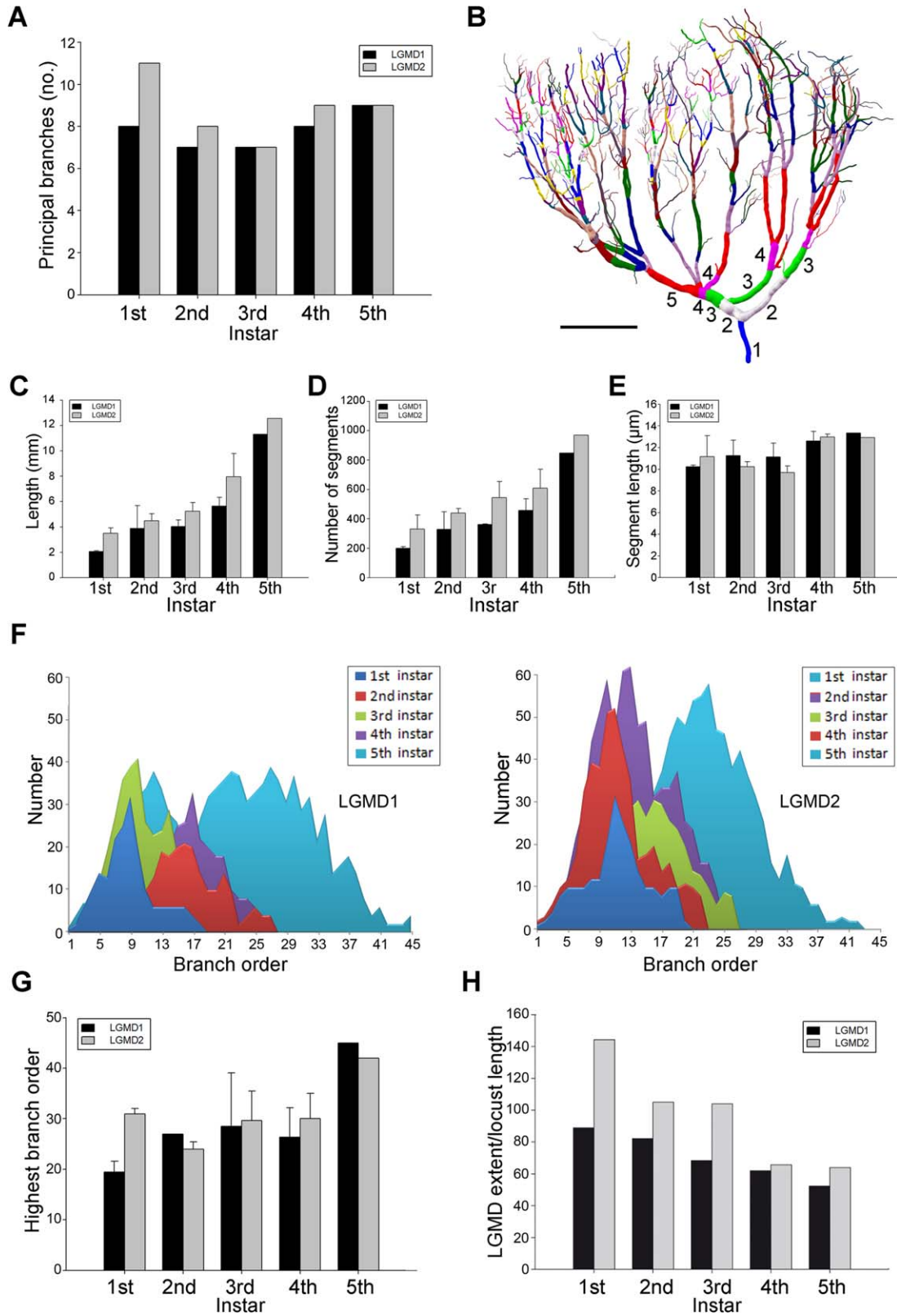
Figure 5

Table 1   Canonical Discriminant Analysis of LGMD1 and LGMD2 Structure Within Each Instar

Neuron	LGMD1			LGMD2		
Discriminant function	1	2	3	1	2	3
% Variance explained	92.7	4.6	2.7	48.9	37.55	13.55
Structural feature (standardized coefficients)						
Branch order	0.223	0.737	0.255	0.545	−0.502	0.792
XY angle	−0.262	0.454	0.387	−0.301	0.579	0.609
Z angle	−0.070	0.123	0.174	−0.050	−0.063	0.028
X	0.355	−0.045	0.011	0.589	0.527	−0.282
Y	0.837	−0.325	0.595	0.742	0.515	−0.438
Z	−0.796	−0.044	0.617	−0.127	−0.777	0.242
Instar (unstandardized coefficients)						
1st instar	−0.382	−0.729	−0.210	−0.922	0.605	0.352
2nd instar	−1.120	0.305	−0.331	−0.118	0.276	−0.558
4th instar	−0.751	0.020	0.238	−0.148	−0.759	0.063
5th instar	2.110	0.071	−0.020	0.920	0.291	0.188

A canonical discriminant analysis applied to the data for the LGMD1 (left columns) and to the data for the LGMD2 (right columns), allowed us categorize the data as coming from a particular instar. The data consisted of six structural measurements from the anatomy of reconstructed LGMD1 and 2 neurons in size matched 1st, 2nd, 4th, and 5th instars. The magnitude and the sign of these coefficients indicate the amount of separation between categories and which instar is being separated from the rest by the function.

Of the two neurons, the LGMD1 showed the greatest change in discriminant function 1 between early and late instars, which suggests that the LGMD1 was initially more rudimentary than the LGMD2 and less like its final form.

While making the dissections needed for this study, we noted that the brains of young locusts are bigger in relation to their body size than those of adults and young animals also have less fat, connective tissue, and muscle surrounding the brain in the head capsule. The same principle is observed if considering the size of the LGMDs. We compared the dorso-ventral extent of the fan-shaped dendritic tree relative to the length of each juvenile locust [Fig. 5(H)]. If we compare a 5th and a 1st instar, the size of the animal increases about 4.2 times while the width of the LGMDs only increases about 2.8 times (LGMD1: 2.61; LGMD2: 2.98). As we draw the borders of the lobula in each of the sections that makes up a reconstruction, we can confirm that the surface covered by the neurons with respect to the neuropil is similar in all instars.

Hiding Behavior

We recorded the responses of 10 animals from each larval stage to an approaching black ball (see details in "Materials and Methods"). During each trial,

Figure 5   Quantification of changes in the morphologies of the LGMD1 and the LGMD2 during larval development. A: The number of principal branches contained in the fan-shaped arborization was counted for the neuron reconstructions shown in Figure 4. B: An example of the colored by branch order analysis of a 4th instar LGMD2. Each branch is colored according to its centripetal order in the tree (a few are numbered as examples). Scale bar: 50 μm. C: Total length (calculated as the sum of the lengths of all the branches in a given tree) was analyzed for all the neural reconstructions that were complete (1st to 5th instar: LGMD1 n = 2, 2, 2, 3, 1; LGMD2 n = 2, 2, 3, 2, 1). D: Number of segments (defined as a portion of a branched structure that is delimited by nodes or terminations and with no intermediate nodes) and (E) mean segment length for each reconstruction. F: With the information derived from the branch order analysis (see B), we constructed histograms for the neuron reconstructions in Figure 4 showing the number of segments in the different branch orders. Left: Branching pattern for LGMD1. Right: Branching pattern for the LGMD2. G: The highest branch order also illustrates the complexity of a tree because numbers are successively assigned to branches to describe the hierarchy of the branching scheme. All the neural reconstructions that were complete were used in this analysis. H: The ratio between the dorso-ventral extent of the fan-shaped arborization of the LGMD and the locust length was calculated for the animals from which the reconstructions shown in Figure 4 were made. Bars show mean ± SE.
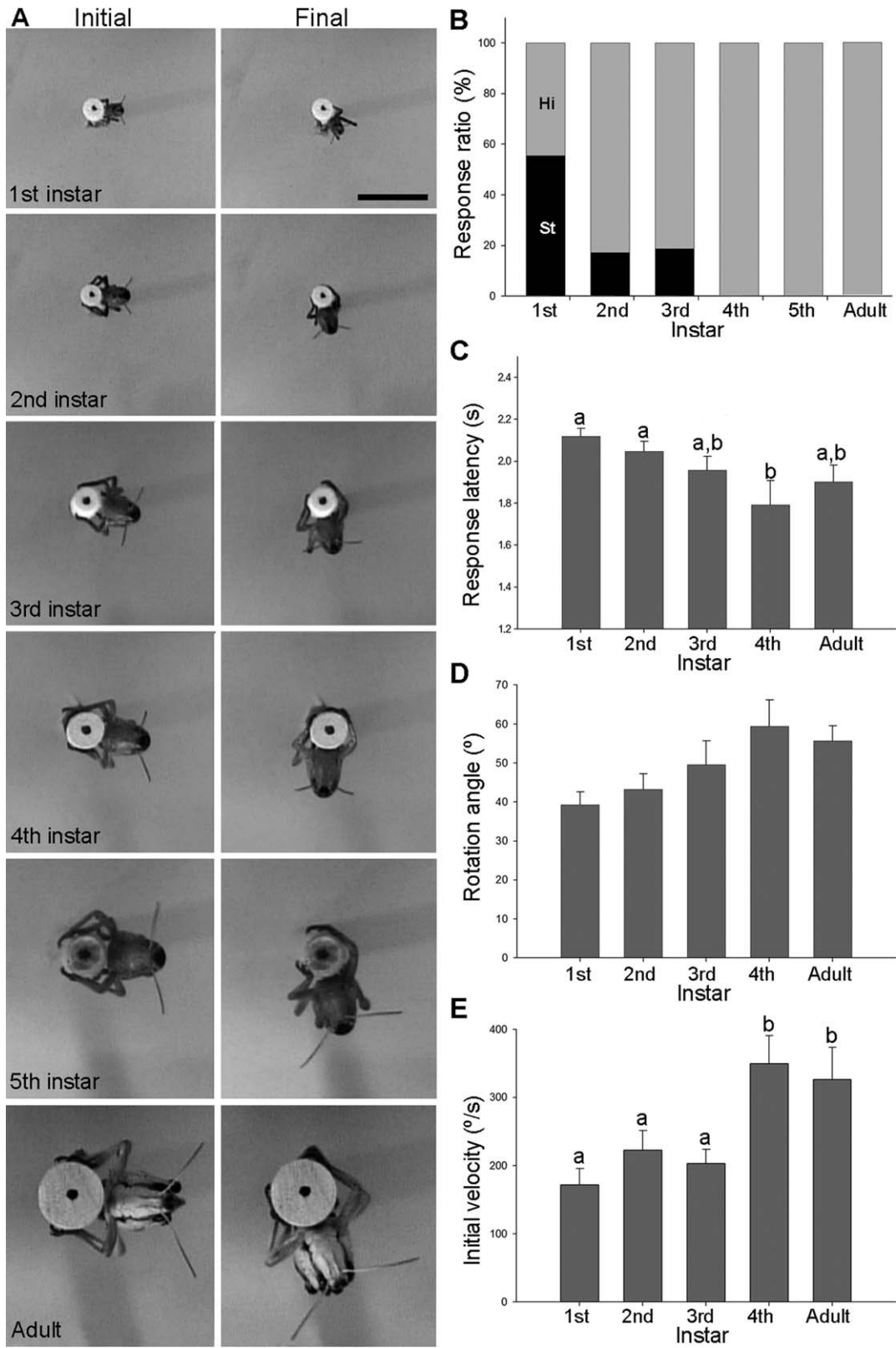
Figure 6

locusts were filmed from above. The type of behavior triggered by the looming stimulus was sorted into three categories: hiding, startle, and no response. A hiding response involved a repositioning behavior in which locusts sitting on a rod turned to hide from an approaching stimulus by moving behind the object. A complete hiding response involved a turn through 90 degrees, to a position in which the rod ended up between the locust and the ball. A startle response consisted of a short, slightly lateral, sudden movement. Some juveniles quickly moved back to the starting position when displaying this response, so the final rotation angle was usually very small or even zero.

In a previous report, 5th instar locusts were found to perform different intensities of hiding responses depending on the angle with which the stimulus was presented and on parameters such as velocity, contrast, and room temperature (Hassenstein and Hustert, 1999). Here, we compared locusts' ability to display escape responses throughout larval development and, therefore, we used only one stimulus (with a fixed velocity, size, color, and direction) to present to all animals. We observed hiding responses in all instars, including 1st instars, less than 1-day old [Fig. 6(A)]. However, some of the younger instars (1st to 3rd instars) sometimes showed a startle response instead. This is likely to be a behavioral choice rather than a developmental constraint because animals displaying startle responses could hide in other trials. Startle responses were not seen in older animals [Fig. 6(B)]. Because the hiding response is performed by all nymphal stages, the following question arises: are the characteristics of such a response similar in all stages of development? By exploring different parameters of the hiding response, we discovered changes in latency and rotation velocity but not angle of movement [Fig. 6(C–E)]. The latency of response changed significantly with developmental stage (Welch Robust Anova: $F(4; 21.58) = 2.658$; $p = 0.035$) becoming shorter as locusts grow and reaching a minimum value for 4th instars. This difference meant that the youngest instars responded to the approaching object later than the older instars, when it subtended a larger angle on the retina but always before the end of the approach [see Fig. 6(C)]. The angle rotated during the hiding response showed a tendency to increase with age, but instar was not a statistically significant factor [Fig. 6(D); One way Anova: $F(4; 42) = 2.423$; $p = 0.063$]. On the other hand, instar had a significant effect on the initial angular velocity of the responses, with the younger instars slower than 4th instars and adults [Fig. 6(E); Welch Robust Anova: $F(4; 20.396) = 3.792$; $p = 0.019$].

The movement of the real ball is subject to acceleration due to gravity and generates nonvisual cues (e.g., mechanical stimulation produced by the movement of the air displaced by the ball). These effects are especially strong in the final part of the approach when younger instars respond. To verify that young instars were using vision to detect the approaching stimulus and to gain more information about hiding responses through development, we used computer-generated looming stimuli. We compared the responses triggered by dark and light looming disks of the same contrast against background in 1st, 3rd, and 5th instars. Computer-generated stimuli were less effective than the real ball in evoking hiding in the locusts and we had to use a slower approach to evoke conspicuous responses (see "Materials and Methods"). Even with this stimulus, a proportion of animals responded to the looming stimulus with a startle response, or did not respond at all [Fig. 7(A)]. This was the case even for 5th instars that had previously responded by hiding when stimulated with the real ball.

Figure 6 Hiding responses are seen throughout development. A: Examples of hiding behavior performed by all the instars (1st instars to adults). Top view images of the locust's position captured at the start of the trial (left column) and after the end of the hiding response (right column). The ball approached from the top of the image. Scale bar: 1 cm. B: Proportion of responses evoked by the looming stimulus in each stage of development. Black bar: startle responses (St). Gray bar: hiding responses (Hi). Number of trials included 1st to adult: 36, 35, 32, 28, 30, 30. C–E: Parameters of the hiding response. Only locusts that responded with a hiding response were considered. C: The latency of response changed significantly with instar (Welch Robust Anova: $F(4; 21.58) = 2.658$; $p = 0.035$) decreasing as juveniles grow (pairwise comparisons *post hoc* by DMS, $p < 0.05$ for 1st vs. 4th and 2nd vs. 4th). D: The angle turned during hiding showed a small increase in successive instars but this factor was not statistically significant (One-way Anova: $F(4; 42) = 2.423$; $p = 0.063$). E: The velocity of response changed significantly with instar stage being the first three developmental stages slower than the older ones (Welch Robust Anova: $F(4; 20.396) = 3.792$; $p = 0.019$; pairwise comparisons *post hoc* by DMS, $p < 0.05$ for 1st vs. 4th; 1st vs. adult; 2nd vs. 4th and 3rd vs. 4th). Bars show mean $\pm$ SE. Different letters stand for significantly different groups.
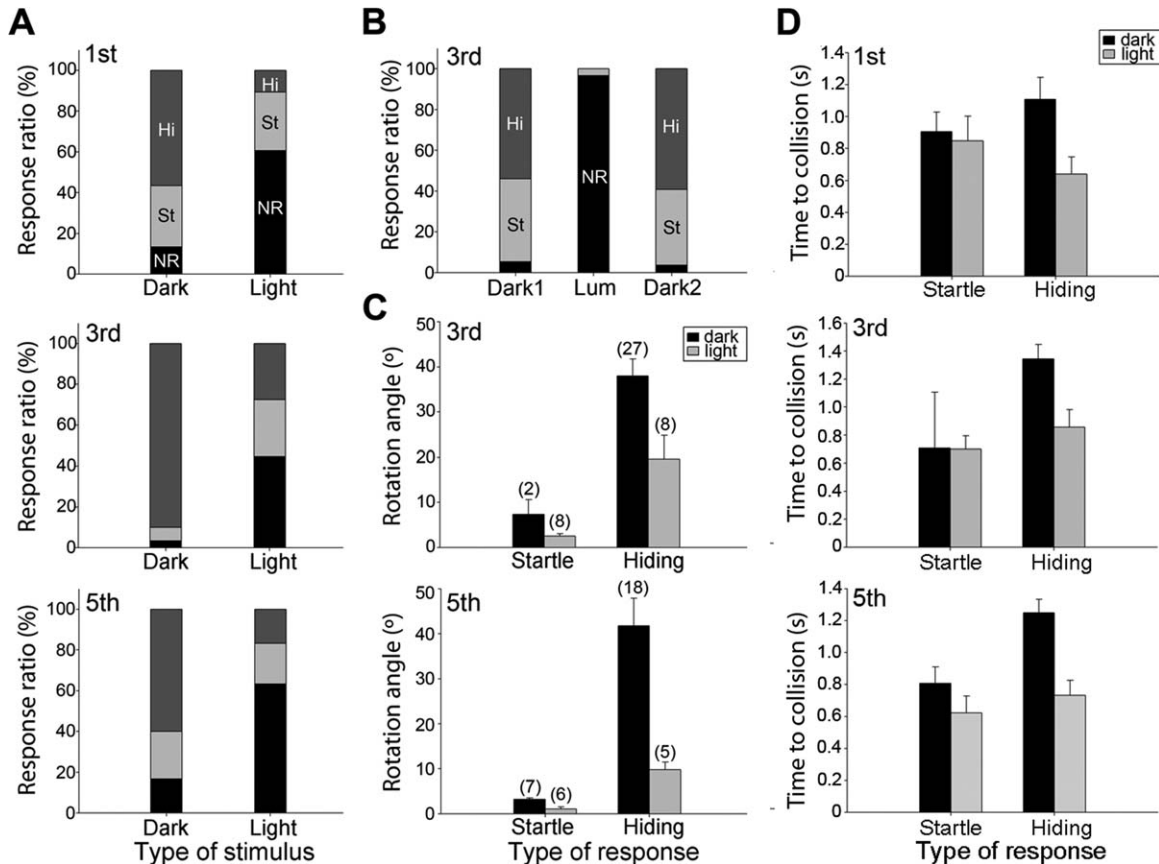
Figure 7 Computer-generated light and dark approaching disks evoke different responses. A: Frequency of performance of different behaviors (no response (NR): black; startle (St): light gray; or hiding (Hi): dark gray) in response to dark and light looms ($n = 10$ locust per instar group, 6 trial repetitions per animal). B: Frequency of performance of different behaviors (no response: black; startle: light gray; or hiding: dark gray) triggered by a dark loom (dark1), by an equivalent luminance decrease stimulus (lum) and by another dark loom (dark2). C: Intensity of response is represented here by the angle of rotation performed. The number of trials with responses in each group is depicted in parenthesis. Data for 3rd and 5th instars is shown. D: Latency of response relative to the time of collision. It is measured as the time the looming ended its expansion minus the frame before a movement of the locust was detected. Each graph displays data from a single developmental stage, the instar group is displayed at the top left corner. Bars show mean $\pm$ SE.

Despite this, the experiment clearly shows that a different behavioral output is obtained when using dark or light stimuli. This difference was consistent across instars because a similar pattern of distribution of responses was observed in all instars [Fig. 7(A)]. In particular, we found that locusts performed a hiding response more frequently when stimulated with a dark object than with a light one (Supporting Information Movies 4–5). In contrast, most of the trials using the light stimulus elicited no response (Supporting Information Movies 6–7). On the other hand, the contrast sign of the stimulus did not seem to systematically affect the probability of displaying a startle response [Fig. 7(A)].

Hiding responses were evoked exclusively by the looming stimulus, in which edges moved, because no hiding responses were recorded when an equivalent luminance change stimulus, with no edge movement, was used [Fig. 7(B)]. To test this lack of response was not simply due to habituation, we recorded the responses of nine 3rd instar locusts to stimulation with a dark looming stimulus (loom 1), then an equivalent luminance decrease stimulus, and then another dark loom (loom 2). We divided the responses into three categories: hiding, startle, and no response [Fig. 7(B)]. The dark looming stimulus (loom 1) triggered mainly hiding but also startle responses [first panel Fig. 7(B)], giving a median overall turning angle of 20 degrees. In contrast, no

hiding and only one startle response was recorded to the luminance change presented alone [second panel Fig. 7(B)], giving a median turning angle of 0 degrees. Loom 2 triggered mainly hiding responses [third panel Fig. 7(B)], with a median overall turning angle of 10 degrees. The angular extent of the hiding responses to looms 1 and 2 were not statistically different (Mann-Whitney Rank Sum Test on non-normal data, $p = 0.727$) but they were both significantly different from the response to luminance decrease alone (Mann-Whitney Rank Sum Test on non-normal data, $p < 0.001$), indicating that the lack of response in the luminance decrease trials was not due to fatigue or habituation but due to the stimulus itself.

Further evidence of the different releasing strength of the dark and light stimuli is that, in general, in trials where hiding occurred, the response was stronger (larger angle of response) when the dark object was used [Fig. 7(C)].

We found a consistent difference in the latencies of the hiding responses triggered by the dark and the light stimuli. Such difference was not present when comparing startle responses. In fact, in all instars tested, the latency of the hiding response was significantly shorter when the dark stimulus was used [Repeated measure ANOVA, Instar factor: $F(2; 9) = 3.563$, $p = 0.072$; Stimulus factor: $F(1; 9) = 24.07$, $p = 0.001$; interaction $F(2; 9) = 3.058$; $p = 0.097$; Fig. 7(D)]. Taking all instars together, the response latencies were 5.27 ± 0.08 s (corresponding to a subtended angle of $24°$) for the dark stimulus and 5.69 ± 0.05 for the light stimulus (corresponding to a subtended angle of $38°$).

DISCUSSION

Holometabolous insects, such as flies and moths, change radically both in shape and in behavior during development. The crawling larva molts into a pupa which over the space of a few days gives rise to a fast flying adult. This implies a complete remodeling of the CNS, involving drastic changes in the intrinsic properties, dendritic architecture, and synaptic interactions of neurons (reviewed in Consoulas et al., 2000; Libersat and Duch, 2002, Meseke et al., 2009). In contrast, the development of hemimetabolous insects, such as the locust, is gradual; first instars' morphology and physiology are very similar to the adults' with only a few distinctions (i.e., they cannot fly like the adults). The question is then, are the brains of 1st instars also small, miniature but functional versions of the adults'? Or do new networks

controlling adult behaviors only develop, when the behavior is actually displayed? Evidence of the former comes from the work of Dagan and Volman (1982) in which they show that first instar cockroaches, with only 2 wind-receptive filiform hairs in each cercus (compared with 200 in the adult) are still able to perform accurate escape responses comparable with those of adults. In locusts too, Bucher and Pflüger (2000) showed that the wind-sensitive interneuron A4I1 has the same general morphological features in all developmental stages and that directional sensitivity is already present in 1st instars. In the locust visual system, the DCMD looks very similar in embryos and adults, undergoing only allometric enlargement (Bentley and Toroian-Raymond, 1981) and is functional in the first instar (Simmons et al., 2013).

There are also no hard and fast rules about the development of adult specific behavior and neuronal circuits. Fully functional neural circuits involved in adult-specific motor patterns have been documented in newly hatched locust nymphs. For example, flight motor activity could be evoked in 1st instar locusts' motor nerves using direct application of octopamine to the thoracic ganglia although the animals are not capable of responding to a wind stimulus with a flight motor output (Stevenson and Kutsch, 1986). Another example in locusts are three auditory neurons (G, B, and C) that show the same general morphology, dynamic properties and synaptology in early instars and adults despite the fact that 1st instars are probably deaf to airborne sound (Boyan, 1983). In contrast, circuits involved in song production and flight in crickets develop gradually during successive molts but are not functional at hatching (Bentley and Hoy, 1970). To summarize, some 1st instars are born with the nervous system ready to perform particular adaptive behaviors accurately while circuits involved in the adult behavioral repertoire develop progressively, and might be subject to silencing by descending inhibition during nymphal stages (Bentley and Hoy, 1970; Anton et al, 2002). Therefore, the maturity of the underlying neural circuitry and the ability to display a behavior are not necessarily correlated. Taking that into account, we studied the ontogeny of escape behaviors triggered by approaching stimuli and of key neurons that could be involved in such responses in *Locusta migratoria*.

Ontogeny of the LGMDs

The capacity to detect looming objects and to act rapidly and appropriately is crucial for the survival of many animals. Most studies have focused on the

structure and function of adult neurons even though collision-avoidance behaviors have been described from the start of an animal's life (e.g., human babies, Bower et al., 1971) and are probably innate or require minimal learning (Fotowat and Gabbiani, 2011). In some cases like *Drosophila*, however, even though the neural pathway underlying the escape response is fully functional at hatching, some form of suppression prevents immature flies from escape looming stimuli in the first couple of hours post-eclosion (Hammond and O'Shea, 2007).

Here, we have described the LGMD1 and the LGMD2 neurons in each larval stage of the locust (even in 1st instar locusts that are about 6 mm long). We combined a classical histological method with a powerful system for three-dimensional neuronal reconstruction so the resulting reconstructions had a quality and detail that allowed an analysis of the changes in the neuronal structure during development. The dramatic shape and morphological constancy of the LGMD neurons (Rind and Simmons, 1998; Rind and Leitinger, 2000) made this approach feasible. The basic structure of the LGMDs seems to be already laid down at hatching because, for example, the number of principal branches was constant throughout development for both neurons and the outline of the neurons was similar in all the instars. We found an allometric enlargement of both dendritic trees during larval development. As was mentioned before, a similar pattern has been described for the DCMD neuron that is postsynaptic to the LGMD1 (Bentley and Toroian-Raymond, 1981) and for other identified neurons (Blagburn and Beadle, 1982; Shankland and Goodman, 1982; Boyan, 1983). However, it is interesting that for the LGMDs, the increase in total length observed in the dendritic structures during development was mainly due to an increase in the number of segments and not to an increase in the mean segment length [Fig. 5(C–E)]. We could not find studies in hemimetabolous insects with detailed enough information about individual neurons to compare these data with. In a holometabolous insect, the moth *Manduca sexta*, motoneuron 5, which in the larva innervates a crawling muscle and in the adult a wing, has two different modes of dendritic growth during its pupal to adult development. The first is a rapid, growth-cone-dependent phase in which new branches are added at order 1–40. In this period, the changes in total dendritic length are correlated with strong changes in the number of segments but with minor changes in the average dendritic segment length. The second phase is growth-cone-independent and involves a slower branching, limited to high-order dendrites and to the perimeter of the

dendritic field (Libersat and Duch, 2002). Even though the development of hemimetabolous insects, such as the locust, is gradual (in contrast to holometabolous postembryonic development with its extensive dendritic regression and then regrowth), two similar phases were evident in the development of the LGMD1 and 2. Like phase 1 in moths, there was a gradual growth in the LGMDs dendrites during the first 4 larval stages and all instars had branch orders with similar frequency distributions and only minor changes in the highest branch order. In 5th instars, there was a large increase in the highest branch order and a shift in the frequency distribution of branch order toward higher orders as found in phase 2 in the moth [Fig. 5(F,G)]. A large change in dendritic development between 4th and 5th instars was also confirmed using a CDA.

Interestingly though, in locusts, the growth of the dendritic trees does not decelerate between 4th and 5th instars, showing a rather constant (or even exponential) increase during all developmental stages that would fit a phase 1 type of growth. We think that this phenomenon is related to the progressive addition of new ommatidia that occurs during postembryonic development and it would involve the concomitant addition of new segments in which the new connections would be established. New ommatidia are added at the anterior edge of the eye and become functional after each moult (Anderson, 1978). In *Locusta migratoria*, the number of ommatidia increases from 2200 in 1st instars to about 8100 in adults (Simmons et al., 2013). Consistent with that, the structural parameter that best separated the morphology of the LGMD1 and LGMD2 in the different instars in the CDA was the *Y* coordinate of each branch point in the main dendritic tree (first discriminant function, Table 1). This coordinate is most closely correlated to the position of the tip of the branches of the fan-shaped arborizations as they develop and has been shown to receive information from the anterior part of the retina in the LGMD1 (Peron et al., 2009), precisely the region were new ommatidia are added in each moult.

In line with the results discussed in this section, we have recently shown that the DCMD neuron from a 1st instar is already capable of distinguishing approaching from receding objects and of discriminating between different approach speeds (Simmons et al., 2013). However, the responses are refined considerably throughout successive instars: the DCMD becomes more selective in its response and the vigor of its responses to looming objects increases, both of which might also be partly explained by the increase in the size and number of ommatidia in the eye.

Brain, Behavior, and Development

To examine the ontogeny of escape behaviors evoked by approaching stimuli, we analyzed the responses triggered by real and computer-generated looming. All locusts responded readily to an approaching dark ball, including those only a few hours post-hatching. Differences in the probability of displaying startle or hiding responses were evident between younger animals and adults, with more hiding responses shown by adult locusts (Fig. 6; $\chi_5^2 = 54.4$, $p < 0.001$; paired comparison by Marascuillo procedure: $p < 0.05$ for 1st vs. 2nd, 3rd, 4th, 5th, and adults).

Certainly, the real ball also stimulates other sensory modalities apart from vision (e.g., mechanoreception). These nonvisual cues become stronger as the ball approaches the locust coinciding with the time younger instars start responding. Therefore, we verified that indeed young instars were using vision to detect the approaching stimulus by using computer-generated stimuli. We tried different velocities and sizes to find the more effective stimulus for triggering hiding behavior. No consistent responses were evoked when using a virtual stimulus with a similar $l/|v|$ to the real ball. The more effective stimulus turned out to be the slowest one we tried with an $l/|v| = 300$ ms, but even with this stimulus we found a greater proportion of trials with no response using the virtual images. Interestingly, and against our predictions, we obtained a similar probability of performing hiding and startle responses in 1st and in 5th instars. Even though many attributes of the stimuli (velocity, sensory modalities targeted, etc.) are different between real and computer-generated looming, it is notable that the relative efficacy of the stimuli for triggering hiding responses changes between instars: for 5th instars, the dark projected stimulus was less salient than the real black ball, because they displayed either startle or no responses in 40% of the trails with computer-generated looming objects compared with 0% with the real approaching ball trials. For younger instars, the computer-generated stimulus seemed more effective than the real ball because 1st and 3rd instars showed a tendency to increase their probability of hiding (from 44 to 57%, and from 81 to 90%, respectively). These differences could be explained by the increase in optical resolution that occurs during development (Simmons et al., 2013). The poorer visual acuity might also explain the delayed hiding responses observed in younger instars [Fig. 6(C)].

Both hiding and startle responses were performed by all nymphal stages although with probabilities that depended both on the locusts' age and the stimulus used. The particular escape strategy selected was not set by developmental constraints, as animals displaying startle responses could hide in other trials. We did, however, find ontogenic changes in the hiding response: its latency got shorter, and its velocity increased, with locust age. Nonetheless, these kinds of changes do not require the presence of new mature elements in the circuitry controlling the response and are consistent with a refinement of neurons and connections already present at hatching.

Are the LGMDs Involved in Hiding Behavior?

Hiding is a robust evasive response displayed by locusts and other grasshoppers to looming stimuli (Hassenstein and Hustert, 1999). The neural pathway generating this response is unknown but since it is triggered by looming stimuli, the LGMDs are good candidates. The neural reconstructions of the LGMDs show that their structure is identifiable in 1st instars though the LGMD2 seems more mature than the LGMD1 because it is the bigger in size (segment number, length, LGMD extent/locust length ratio) and complexity (branching pattern, highest branch order). CDA analysis also supports this maturity of the LGMD2 at hatching when, of the two LGMDs, it is closest to the 5th instar neuron in structure. However, we know from physiological experiments that the LGMD1 (read through the DCMD output) is capable of detecting approaching stimuli in newly hatched instars (Simmons et al., 2013). Therefore, both LGMD neurons are potential candidates for being involved in the hiding response circuit. The experiments performed with virtual stimuli revealed very few hiding responses to the light stimulus but strong and consistent hiding responses in all instars to the dark stimulus (Fig. 7). The number of trials without a response was very high when using the light stimulus but low when using the dark one. In the adult, a difference in the stimulus preference of the LGMDs has been reported: a light looming stimulus does not excite the LGMD2 but does excite the LGMD1 (Simmons and Rind, 1997). If such response preferences were similar in younger instars, then the clear difference in the effectiveness of the two stimuli would suggests a role for the LGMD2 neuron in triggering the hiding response. Further experiments both in juveniles and adult locusts will be necessary to prove such a hypothesis.

REFERENCES

Anderson H. 1978. Postembryonic development of the visual system of the locust, *Schistocerca gregaria*. I. Patterns of growth and developmental interactions in the retina and optic lobe. J Embryol Exp Morphol 45:55–83.

Anton S, Ignell R, Hansson BS. 2002. Developmental changes in the structure and function of the central olfactory system in gregarious and solitary desert locusts. Microsc Res Tech 56:281–291.

Barth M, Hirsch HV, Meinertzhagen IA, Heisenberg M. 1997. Experience-dependent developmental plasticity in the optic lobe of *Drosophila melanogaster*. J Neurosci 17:1493–1504.

Bastiani M, Pearson KG, Goodman CS. 1984. From embryonic fascicles to adult tracts: Organization of neuropile from a developmental perspective. J Exp Biol 112:45–64.

Bentley D, Toroian-Raymond A. 1981. Embryonic and postembryonic morphogenesis of a grasshopper interneuron. J Comp Neurol 201:507–518.

Bentley DR, Hoy RR. 1970. Postembryonic development of adult motor patterns in crickets: A neural analysis. Science 170:1409–1411.

Blagburn JM, Beadle DJ. 1982. Morphology of identified cercal afferents and giant interneurones in the hatchling cockroach *Periplaneta americana*. J Exp Biol 97:421–426.

Bower TGR, Broughton JM, Moore MK. 1971. Infant responses to approaching objects: An indicator of response to distal variables. Percept Psychophys 9:193–196.

Boyan GS. 1983. Postembryonic development in the auditory system of the locust: Anatomical and physiological characterisation of interneurones ascending to the brain. J Comp Physiol A 151:499–513.

Bucher D, Pflüger H. 2000. Directional sensitivity of an identified wind-sensitive interneuron during the postembryonic development of the locust. J Insect Physiol 46:1545–1556.

Consoulas C, Duch C, Bayline RJ, Levine RB. 2000. Behavioral transformations during metamorphosis: Remodeling of neural and motor systems. Brain Res Bull 53:571–583.

Dagan D, Volman S. 1982. Sensory basis for directional wind detection in first instar cockroaches, *Periplaneta americana*. J Comp Physiol 147:471–478.

Fotowat H, Fayyazuddin A, Bellen HJ, Gabbiani F. 2009. A novel neuronal pathway for visually guided escape in *Drosophila melanogaster*. J Neurophysiol 102:875–885.

Fotowat H, Gabbiani F. 2007. Relationship between the phases of sensory and motor activity during a looming-evoked multistage escape behavior. J Neurosci 27:10047–10059.

Fotowat H, Gabbiani F. 2011. Collision detection as a model for sensory-motor integration. Annu Rev Neurosci 34:1–19.

Fotowat H, Harrison RR, Gabbiani F. 2011. Multiplexing of motor information in the discharge of a collision detecting neuron during escape behaviors. Neuron 69:147–158.

Gabbiani F, Krapp HG, Koch C, Laurent G. 2002. Multiplicative computation in a visual neuron sensitive to looming. Nature 420:320–324.

Gray JR, Blincow E, Robertson RM. 2010. A pair of motion-sensitive neurons in the locust encode approaches of a looming object. J Comp Physiol A 196:927–938.

Heisinger PR, Zhai RG, Zhou Y, Koh TW, Mehta SQ, Schulze KL, Cao Y, Verstreken P, Clandinin TR, Fischbach KF, Meinertzhagen IA, Bellen HJ. 2006. Activity-independent prespecification of synaptic partners in the visual map of Drosophila. Curr Biol 16:1835–1843.

Hammond S, O'Shea M. 2007. Ontogeny of flight initiation in the fly *Drosophila melanogaster*: Implications for the giant fibre system. J Comp Physiol A 193:1125-1137.

Hassenstein B, Hustert R. 1999. Hiding responses of locusts to approaching objects. J Exp Biol 202:1701–1710.

Hatsopoulos N, Gabbiani F, Laurent G. 1995. Elementary computation of object approach by wide-field visual neuron. Science 270:1000–1003.

Karmeier K, Tabor R, Egelhaaf M, Krapp HG. 2001. Early visual experience and the receptive-field organization of optic flow processing interneurons in the fly motion pathway. Vis Neurosci 18:1–8.

Leitch B, Shepherd D, Laurent G. 1995. Morphogenesis of the branching pattern of a group of spiking local interneurons in relation to the organisation of embryonic sensory neuropils in locust. Philos Trans R Soc London B 349:433-447.

Libersat F, Duch C. 2002. Morphometric analysis of dendritic remodeling in an identified motoneuron during postembryonic development. J Comp Neurol 450:153–166.

Meinertzhagen IA. 1976. The organization of perpendicular fibre pathways in the insect optic lobe. Philos Trans R Soc London B 274:555–594.

Meseke M, Evers JF, Duch C. 2009. Developmental changes in dendritic shape and synapse location tune single-neuron computations to changing behavioral functions. J Neurophysiol 102:41–58.

Nakagawa H, Hongjian K. 2010. Collision-sensitive neurons in the optic tectum of the bullfrog, *Rana catesbeiana*. J Neurophysiol 104:2487–2499.

O'Shea M, Williams JLD. 1974. The anatomy and output connection of a locust visual interneurone; the lobular giant movement detector (LGMD) neurone. J Comp Physiol 91:257–266.

Peron SP, Jones PW, Gabbiani F. 2009. Precise subcellular input retinotopy and its computational consequences in an identified visual interneuron. Neuron 63:830–842.

Peron SP, Krapp HG, Gabbiani F. 2007. Influence of electrotonic structure and synaptic mapping on the receptive field properties of a collision-detecting neuron. J Neurophysiol 97:159–177.

Pflüger HJ, Hurdelbrink S, Czjzek A, Burrows M. 1994. Activity-dependent structural dynamics of insect sensory fibers. J Neurosci 14:6946–6955.

Preuss T, Osei-Bonsu PE, Weiss SA, Wang C, Faber DS. 2006. Neural representation of object approach in a decision-making motor circuit. J Neurosci 26:3454–3464.

Raper JA, Bastiani M, Goodman CS. 1983a. Pathfinding by neuronal growth cones in grasshopper embryos. I. Divergent choices made by the growth cones of sibling neurons. J Neurosci 3:20–30.

Raper JA, Bastiani M, Goodman CS. 1983b. Pathfinding by neuronal growth cones in grasshopper embryos. II. Selective fasciculation onto specific axonal pathways. J Neurosci 3:31–41.

Rencher AC. 1992. Interpretation of canonical discriminant functions, canonical variates, and principal components. Am Stat 46:217–225.

Rind FC. 1984. A chemical synapse between two motion detecting neurones in the locust brain. J Exp Biol 110: 143–167.

Rind FC. 1987. Non-directional, movement sensitive neurones of the locust optic lobe. J Comp Physiol 161:477–494.

Rind FC. 1996. Intracellular characterization of neurons in the locust brain signaling impending collision. J Neurophysiol 75:986–995.

Rind FC, Leitinger G. 2000. Immunocytochemical evidence that collision sensing neurons in the locust visual system contain acetylcholine. J Comp Neurol 423:389–401.

Rind FC, Santer RD. 2004. Collision avoidance and a looming sensitive neuron: Size matters but biggest is not necessarily best. Proc Biol Sci 271 (Suppl 3):S27–S29.

Rind FC, Simmons PJ. 1992. Orthopteran DCMD neuron: A reevaluation of responses to moving objects. I. Selective responses to approaching objects. J Neurophysiol 68: 1654–1666.

Rind FC, Simmons PJ. 1998. Local circuit for the computation of object approach by an identified visual neuron in the locust. J Comp Neurol 395:405–415.

Rowell CHF. 1971. The orthopteran descending movement detector (DMD) neurones: A characterisation and review. Z Vergl Physiol 73:167–194.

Rybak J, Meinertzhagen IA. 1997. The effects of light reversals on photoreceptor synaptogenesis in the fly *Musca domestica*. Eur J Neurosci 9:319–333.

Santer RD, Rind FC, Stafford R, Simmons PJ. 2006. Role of an identified looming-sensitive neuron in triggering a flying locust's escape. J Neurophysiol 95:3391–3400.

Santer RD, Simmons PJ, Rind FC. 2005. Gliding behaviour elicited by lateral looming stimuli in flying locusts. J Comp Physiol A 191:61–73.

Santer RD, Yamawaki Y, Rind FC, Simmons PJ. 2008. Preparing for escape: An examination of the role of the DCMD neuron in locust escape jumps. J Comp Physiol A 194:69–77.

Schlotterer GR. 1977. Response of the locust descending movement detector neuron to rapidly approaching and withdrawing visual stimuli. Can J Zool 55:1372–1376.

Sehnal F. 1985. Morphology of insect development. Annu Rev Entomol 30:89–109.

Shankland M, Goodman CS. 1982. Development of the dendritic branching pattern of the medial giant interneuron in the grasshopper embryo. Dev Biol 92:489–506.

Simmons PJ, Rind FC. 1992. Orthopteran DCMD neuron: A reevaluation of responses to moving objects. II. Critical cues for detecting approaching objects. J Neurophysiol 68:1667–1682.

Simmons PJ, Rind FC. 1997. Responses to object approach by a wide field visual neurone, the LGMD2 of the locust: Characterization and image cues. J Comp Physiol A 180: 203–214.

Simmons PJ, Sztarker J, Rind FC. 2013. Looming detection by identified visual interneurons during larval development of the locust *Locusta migratoria*. J Exp Biol 216: 2266–2275.

Stevenson PA, Kutsch W. 1986. Basic circuitry of an adult-specific motor program completed with embryogenesis. Naturwissenschaften 73:741–743.

Sun H, Frost BJ. 1998. Computation of different optical variables of looming objects in pigeon nucleus rotundus neurons. Nat Neurosci 1:296–303.

Sztarker J, Strausfeld NJ, Tomsic D. 2005. Organization of optic lobes that support motion detection in a semiterrestrial crab. J Comp Neurol 493:396–411.

Wright GA, Lutmerding A, Dudareva N, Smith BH. 2005. Intensity and the ratios of compounds in the scent of snapdragon flowers affect scent discrimination by honeybees (*Apis mellifera*). J Comp Physiol A 191:105–114.